Structural Changes of Casein Micelles in a Calcium Gradient Film

Ronald Gebhardt*[†] , Manfred Burghammer[†] , Christian Riekel[†],

Stephan Volkher Roth[‡] , and Peter Müller-Buschbaum[⊥]

[†] European Synchrotron Radiation Facility, BP 220, F-38043 Grenoble Cedex 09, France

[‡] HASYLAB at DESY, Notkestr. 85, 22603 Hamburg, Germany

[⊥] TU München, Physik-Department, LS E13, James-Franck-Str.1, 85747 Garching, Germany

European Synchrotron Radiation Facility ESRF - ID13
6, rue J. Horowitz
IBP220, Grenoble 38043 France
Tel.: 0033 (0)476882952
Fax : 0033 (0)476882904
email: ronald.gebhardt@esrf.fr

*Author to whom correspondence should be addressed. email: ronald.gebhardt@esrf.fr

Keywords: casein micelles, proteins, solution casting, µGISAXS, biomineralization

Summary

Calcium gradients are prepared by piling a micropipette with casein solutions of varying calcium concentration and spreading them on glass slides. The casein film is formed by solution casting process which results in a macroscopically rough surface. We used microbeam grazing incidence small-angle X-ray scattering to investigate the lateral size distribution of three main components in casein films: casein micelles, casein mini-micelles and micellar calcium phosphate. At length scales within the beam size the film surface is flat and detection of size distribution in a macroscopic casein gradient becomes accessible. The model used to analyze the data is based on a set of three log-normal distributed particle sizes. Increasing calcium concentration causes a decrease in casein micelle diameter while the size of casein mini-micelles increases and micellar calcium phosphate particles remain unchanged.

Introduction

Casein micelles are colloidal particles of spherical shape with an average diameter of about 100 nm.[1] Their polydispersity can be approximated by a log-normal-distribution.[2] The casein micelle of bovine milk consists of four different phosphor-proteins which can be divided into two groups: the calcium insensitive κ-casein and the calcium sensitive α_{S1}-, α_{S2}- and β-caseins. While the self-associating behaviour of individual caseins in aqueous solution has been well investigated,[3,4] the micellar substructure of casein micelles are still the subject of debate.[5,6,7,8,9] Evidence for a substructured casein micelle surface, probably introduced by calcium phosphat/casein nanoclusters, was found by high-resolution field-emission scanning electron micrographs[10] and more recently using AFM in a liquid cell.[11] It is generally accepted that the stability of casein micelles is ensured by an outer hairy layer of κ-caseins.[12,13]

The main physiological task of caseins is calcium transfer from the mammary gland to the newborn during lactation – needed for the calcification of teeth and bones. Calcium is actively concentrated in the Golgi compartment of mammary cells[14,15] and subsequently assembled as colloidal calcium phosphate within the casein micelles.[16,17] Together with a minor ionized part, the micellar calcium is then secreted into milk. Two thirds of calcium remains in the colloidal state, either bound on the phosphate or carboxyl groups of caseins or incorporated into micellar calcium phosphate particles.[18] The particles are distributed within the casein micelle and are linked to casein phosphate centres. Different structural methods have shown that micellar calcium phosphate particles are several nanometers in size.[19]

Grazing incidence small-angle x-ray scattering is an advanced method for the structural and morphological characterisation of protein films.[20] Compared with other surface sensitive biophysical probes like atomic force microscopy[21,11] or electron microscopy,[6,10] grazing incidence small-angle x-ray scattering is a nondestructive technique with high sensitivity and

statistical relevance. Crystal growth and nucleation induced by highly ordered protein nanotemplates were recently investigated.[22,23,24]

Substructures in casein films prepared using a spin coating technique were first investigated by Müller-Buschbaum P. et al.[25] pH dependent size changes in bulk-like films were found to match with the results obtained in solution. Similar investigations were recently published for calcium concentration dependence.[26] Calcium changes the colloidal properties of casein micelles by neutralizing negatively charged phosphoserin residues and carboxylic groups.[27,28] A subsequent increase in hydrodynamic radius was found in previous experiments in casein solutions.[29] On the contrary, a decrease of casein micelles sizes and an increase in casein mini-micelles were obtained in casein films prepared with a spin coating technique.[26] The results were explained within the framework of an adhesive hard sphere model.[2,30]

In this work, structural changes of casein components are explored in a calcium gradient film. This builds upon previous studies on casein films with a varying calcium concentration prepared by spin coating technique. As an extension, the casein film is prepared by a solution casting technique, which allows a gradient to be introduced for GISAXS study using a micrometer sized beam. Furthermore, the experimental setup provides a range of higher q-values that also allow observations on length scales in the range of the micellar calcium phospate nanoparticles. With a developed form factor model which takes into account the multiple length scale of the casein substructures, the changes in mean size and size distributions of film substructures in the calcium gradient are analysed and discussed.

Experimental Part

Sample Preparation. Casein micelles from commercial-grade skimmed milk were extracted by combined uniform transmembrane pressure micro-filtration (mean pore diameter: 0.1 µm) and ultra-filtration, concentrated by five washing steps and dried in a spraying tower.[31] Caseins (40 mg/ml) were dissolved in filtered 0.1 M Tris/Mes-HCl buffer solution. A pH of 7.3 was adjusted by mixing different volumes of the buffer components. Different amounts of $CaCl_2$ salt were added to prepare seven casein solutions with varying calcium concentrations in the range of 0 to 60 mM in steps of 10 mM. All solutions were equilibrated by thoroughly stirring for 5 h.

The preparation of calcium gradient casein film is illustrated in Fig.1. As a substrate, pre-cleaned glass slides (26x76x0.15 mm^3, Menzel Gläser, Braunschweig, Germany) were used. Details of the cleaning procedure can be found elsewhere.[25] Starting with the sample without calcium, casein solutions with increasing calcium concentration were taken up stepwise by a micropipette and transferred onto the glass surface. For the preparation of the gradient, the solution was slowly pushed out by moving the pipette needle along the long side of the glass slide. The sample preparation protocol was tested using colored ink prior to actual sample preparation. This ensured the optimum transfer of the gradient within the pipette onto the glass surface.

Micro beam Grazing incidence small angle x-ray scattering

The sample is located in the x-y-plane (see Fig.1). The incoming beam k is directed along the x-axis and impinges onto the sample at an incident angle αi. The components qy and qz of the scattering vector q are functions of the angles αi, αf and ψ:

$$q_{y,z} = \frac{2\pi}{\lambda}\begin{bmatrix} \sin\psi\cos\alpha_f \\ \sin\alpha_f + \sin\alpha_i \end{bmatrix} \qquad \text{Equation (1)}$$

They define the reciprocal space coordinate system. The beam is specularly (qy=0, qz>0) and diffusely (qy ≠ 0) scattered. The specular peak and the so-called Yoneda Peak are characteristic patterns of the GISAXS signal.[32] The specular peak appears if the specular condition is fulfilled (αi=αf). The Yoneda Peak occurs at the critical angle of the sample αc, arising from an interference effect of the incident and scattered field.

For understanding the two-dimensional intensity distribution an assembly of several vertical and horizontal slices can be taken into consideration.[33] Lateral structures (perpendicular to the z-axis) of the film surface can be studied by analyzing intensity distributions in the qy direction. Information about the morphology vertical to the sample surface (height of structures, thickness of correlated multilayers) can be extracted from the qz dependence of the scattering signal (detector plot). Further detailed information of GISAXS as a technique for characterizing nanostructured polymer films can be found elsewhere.[20]

Synchrotron Radiation Experiments

Micro beam Grazing incidence small angle x-ray scattering (μGISAXS) experiments were conducted at the ID13 microfocus beamline[34] of the European Synchrotron Radiation Facility in Grenoble, France. The incoming monochromated beam (λ = 0.976 Å) was focused by a Kirkpatrick-Baez (KB) mirror system onto the sample position, which results in high real-space resolution.[34] A micro-ionisation chamber with a 20 μm guard aperture was used to monitor beam intensity and reduce stray radiation. At the focal spot position the beam size was 1x1 μm^2. Due to the incident angle of αi = 0.68º, the footprint of the X-ray beam on the sample is extended 70 μm along the beam direction for geometric reasons. The sample was placed on a two-axis goniometer (α,ψ), mounted on a x/y/z translation unit with 200 nm positional repeatability.[35] In order to find the optimum conditions for μGISAXS on the film surface, each data set consisted of a vertical scan through the sample thickness at a fixed position in the calcium gradient. For this, the height of the sample was changed over a

distance of 350 µm in steps of 5 µm, giving rise to a set of 70 scattering patterns. A MAR165 CCD detector (78.94 µm * 78.94 µm pixel size; 2K*2K pixels; 16 bit readout) was used to record the GISAXS signal. The sample-to-detector distance was 802 mm, determined by a dry rat tail collagen sample.

Data analysis

In order to analyze the GISAXS signal, so-called out of plane cuts can be carried out.[20] Horizontal q_y-cuts of the two-dimensional (q_y,q_z) intensity distribution were taken at the critical angle for casein[25] using the FIT2d software package.[36] Because this work focuses on very thick films an incident angle above the critical angle was chosen. The scattering data was analyzed in a simplified approach assuming only scattering contributions. Additional higher terms including scattering and reflection were omitted. Thus scattering data was analyzed using a composed hard sphere form factor model with log-normal distributed radii. The scattering function I(q) for polydisperse spheres with different radii and volumes is given by:

$$I(q,R) = c \cdot \int_0^\infty V^2(R) \cdot S(q,R) \cdot P(R) dR . \qquad \text{Equation (2)}$$

Here a constant c accounts for the number of scattering particles and the scattering contrast, V is the particle volume.

The single particle structure factor for a sphere is given by:

$$S(q,R) = \left[3 \frac{\sin(q \cdot R) - q \cdot R \cdot \cos(q \cdot R)}{(q \cdot R)^3} \right]^2 , \qquad \text{Equation (3)}$$

The single particle structure factor for a cylinder is given by:

$$S(q,R) = \int_0^{2\pi} \frac{\sin^2\left(q \cdot \frac{L}{2} \cdot \cos(\beta) \right)}{\left(q \cdot \frac{L}{2} \right)^2 \cdot \cos^2(\beta)} \cdot \frac{4 \cdot J_1^2 \cdot (q \cdot R \cdot \sin(\beta))}{q^2 \cdot R^2 \cdot \sin^2(\beta)} \cdot \sin(\beta) d\beta , \qquad \text{Equation (4)}$$

J1 is the first order Bessel function.

The formula for the log-normal distribution is:

$$P(R) = \frac{1}{\sqrt{2\pi}} \cdot \frac{1}{R \cdot \sigma} \cdot e^{-\left(\frac{\ln\left(\frac{R}{R_m}\right)^2}{2\sigma^2} \right)}, \quad \int_{R=0}^{\infty} P(R) dR = 1 \qquad \text{Equation (5)}$$

For data analysis, we used a model containing three log-normally distributed radii (casein micelle; index M, casein mini-micelle; index S, and calcium phosphate; index C, which stand in fractional relation to each other via

$$I_G(q,R) = \frac{1}{1+s+c} \cdot I_M(q,R_M) + \frac{s}{1+s+c} \cdot I_S(q,R_S) + \frac{c}{1+s+c} \cdot I_C(q,R_C) + B, \qquad \text{Equation (6)}$$

and a q-independent background B.

Results and Discussion

A. µGISAXS of casein films prepared by solution casting

In contrast to bulk-like but significantly thinner casein films prepared by spin-coating,[25] solution casting typically results in very thick films. The estimated thickness of the used casein films was several hundred micrometers. On the one hand, this considerable thickness causes difficulties in finding proper conditions for a µGISAXS alignment. On the other hand it allows additional transmission experiments to be carried out. To find the conditions for µGISAXS on the film surface, height scans at a fixed position in the calcium gradient were performed. Fig. 2 depicts the detected 2D intensity signal and a simplified illustration of the underlying scattering process at two representative positions of the height scan. In the first position the beam is focused on the sample's surface resulting in a µGISAXS alignment (Fig. 2, left side). In this case the Yoneda peak is shown as a typical intensity enhancement in the

2D intensity distribution. In the second position the beam enters from the side through the thick casein film and its focus lies within the casein film (Fig. 2, right side). No Yoneda peak is observed and a typical transmission signal dominates the 2D intensity signal. This contribution is exhibited in all scattering patterns collected during the height scan which do not match the µGISAXS alignment. An explanation of the observed scattering profile is represented schematically in Fig. 2 c,d. This shows that if the X-ray beam is focused on the surface, the incident, reflected and transmitted X-ray fields interfere coherently. In this case the Yoneda peak appears at the critical angle. Meanwhile, no enhancement of the transmitted beam can be observed if the beam is focused within the casein film. In this geometry the X-ray beam is scattered but not reflected, which leads to a lack of the Yoneda peak. The remaining scattering contribution originates from a well defined structural spacing inside the bulk of the casein film, as it is known from classical small angle x-ray scattering (SAXS).

B. Line cuts through the µGISAXS intensity distribution

The data analysis is restricted to the µGISAXS signal, which presents the structure of the casein micelles near to the surface as well as in the bulk of the thick casein film. Typical GISAXS cuts from 2D intensity distribution at varying position along the calcium gradient surface are shown in Fig.3 a. The intensity is plotted versus the q_y component of the scattering vector q in a double logarithmic plot. For clarity, the scattering curves are shifted along the y-axis. The model fits are represented by solid lines. Calcium concentration varies in the measurements from the bottom to the top as 0, 5, 10, 15, 30, 35, 40, 55, and 60 mM. The scattering curves show no well pronounced peaks. This can be attributed to polydispersity of the casein compounds, as previously observed from dynamic light scattering experiments.[37,38] Instead of peaks, three characteristic shoulders (marked with arrows) can be seen. The shoulder at q = 1 nm^{-1} doesn't change with varying calcium concentration. The slope of the curve is linked to the width of the size distribution and also remains unchanged.

According to our modeling approach, this shoulder can be related to the sizes of micellar calcium phosphate particles. A similar feature was previously found in the high q region of small angle x-ray profiles.[39] It was recently shown in pH dependent scattering experiments that this shoulder is linked to micellar calcium phosphate.[40]

A second shoulder at q = 0.2 nm^{-1}, which can be attributed to casein mini-micelles, becomes more pronounced with increasing calcium concentration. In this case the slope becomes steeper and the q_y-position shifts towards smaller values. Finally, at calcium concentrations higher than 40 mM, a third shoulder is manifested at q = 0.03 nm^{-1} and belongs to a third size in the film which corresponds to the casein micelles.

C. Particle Sizes

All curves were analysed using the form factor model (Equation 6) described above. Prior to modeling, all scattering curves were normalized at high q (q = 0.001 nm^{-1}). The fits show a good correlation with the experimental data. Fig. 4 depicts the obtained parameter for mean sizes of casein micelles, casein mini-micelles and micellar calcium phosphate particles. For variation of casein micelle sizes in the calcium gradient only approximate values can be given because the information in the GISAXS-pattern is close to the experimental resolution. At low calcium concentrations (up to 30 mM) the radial size has to be extracted from the slope at q < 0.04 nm^{-1}. Good fitting results could be achieved with casein micelle dimensions D > 100 nm. At calcium concentrations higher 40 mM, the slope in the scattering curve is more pronounced and shifted to higher q-values. In this concentration range casein micelle sizes of D = 50 nm are found, as shown in Fig. 4.

In the 0.07 – 0.2 nm^{-1} region of the µGISAXS curve a shoulder is pronounced. A similar structural feature in the scattering curve was derived from previous neutron scattering experiments and considered either as mean sizes of casein submicelles[41] or as the mean spacing of calcium phosphate nanocluster–like particles within the casein micelle.[8] However,

to explain the well-established correlation length in our experimental result, it was necessary to consider an additional structural feature. We found in previous casein film and solution studies casein particles of rather similar sizes which are in coexistence with casein micelles. These so-called mini-micelles are able to aggregate further after addition of calcium.[26,11] Without calcium the slope of the shoulder is small, corresponding to broadly distributed sizes around D = 10 nm. With increasing calcium concentrations the slope becomes steeper, while the q-position shifts to smaller values. This implies an increase in size, as shown in Fig. 4. At high calcium concentrations the mean casein mini-micelle sizes have doubled to D = 20 nm. The sizes of casein micelles and mini-micelles are roughly half of those found in previous experiments in thin casein films.[26] It may be assumed that the small deviations in the size of casein micelle and mini-micelles compared to those reported in the previous study arise due to the use of a different batch of casein as well as the different film preparation method.

Sizes corresponding to the shoulder in the scattering curve at q= 1 nm^{-1}, are also displayed in Fig. 4 as a function of calcium concentration. Over the whole calcium concentration range no variation was observed. The most frequent sizes are distributed around a mean diameter of D = 1 nm. For this part of the scattering curve especially, better fitting results could be achieved by replacing the spherical form factor by a cylindrical form factor in the model. In this case a diameter of D = 1.9 nm and a height of 1.5 nm was obtained for the cylinder. The values of both model fits are in the range of sizes which were found for artificial preparations of milk calcium phosphate particles.[42] The authors found a granular diameter of 2.5 nm when performing electron microscopy on wet and freeze-dried ultra filtrate calcium phosphate precipitates.

D. Size Distributions

From the obtained fitting parameters, size distributions of the three casein components were calculated. Their continuous variation over the whole calcium gradient is shown as a contour

plot in Fig.5. For discussion, two size distributions are displayed at 0 mM and 60 mM calcium, respectively (Fig.6).

In the case of the micellar calcium phosphate particles' distribution (Fig.6, left), no changes were observed within the calcium gradient. The particle size distributions between 0 mM and 60 mM show a similar shape and width. It is known from experiments investigating the exchangeability of calcium, that colloidal calcium phosphate in casein micelles and free diffusible calcium are partly exchangeable.[43] In the studied calcium gradient film, the exchangeability between both phases was guaranteed by the used gradient film technique (see sample preparation). This suggests that there are no calcium-induced structural changes on a scale of between 1-3 nm in casein micelles. Aoki et al[44] found that for artifical casein micelle formation, the amount of casein aggregates cross–linked by micellar calcium phosphate depends upon the micellar calcium and phosphate concentration, which can be increased by adding calcium. Since no evidence for structural changes of micellar calcium phosphate was found in this study, this effect might be explained by an increase in the number of particles.

The distributions of casein mini-micelle sizes are shown in Fig.6, center. At 0 mM, the sizes are narrowly distributed around a mean value of D = 10 nm. At 60 mM calcium, the distribution is broader and shifted towards mean sizes of D = 21 nm. As known from casein solutions, mini-micelles, casein micelles and their constituents are in equilibrium with each other.[45] Casein monomers are able to aggregate due to their self-associating capability. Calcium binding to negatively charged caseins supports growth by diminishing electrostatic repulsion forces, which enhances hydrophobic contacts. Averaged sizes in the range of between 10–20 nm were reported for micelle-like aggregates of β- and κ-casein.[46] A size increase of the casein mini-micelles was found if calcium was added to the solution.[38]

Compared to the casein mini-micelles, the distributions of casein micelle sizes show an opposite effect. Under the influence of calcium, the micelle distribution becomes sharper and shifts towards smaller radii. In contrast, dynamic light scattering experiments in solution show

an increase in the mean hydrodynamic radius and distribution width.[41,29,26] An explanation for this difference is based upon the variation in the sensitivity of the methods used and the high polydispersity of the sample. In the dynamic light scattering experiment, a minor number of large particles strongly biased the scattering signal. The detection probability of these aggregates in the light scattering experiment is further enhanced due to the longer temporary (several minutes) and broader spatially averaging (detection volume approx. 1 mm^3) of the technique. In the μGISAXS experiments presented here, there was no evidence for the formation of casein micelle aggregates.

The calcium effect on casein micelles is thought to proceed in two phases. First, caseins become incorporated in the casein micelle. Calcium neutralizes negative charged phosphoserin residues and carboxylic groups and reduces repulsion forces between caseins. This leads to an increase in molecular weight without size changes. In a second step, larger amounts of calcium increase the radius of the casein micelles. The collapse of the stabilizing hairy κ-casein layer on the casein micelle surface is thought to be the reason for this aggregation process. The critical calcium concentration at which flocculation and gel-formation starts, was found to be larger than 100 mM, and therefore higher than the concentrations used in the experiments reported within this study.

It has been recently shown [26] that an intermediate phase exists in which the presence of calcium decreases the size of casein micelles. The addition of calcium reduces the negative charges of κ-casein and the polyelectrolyte brush loses its extended conformation. In this state the size of the hairy κ-casein layer is diminished but not fully collapsed. In spin coated casein films, where the micelles are closely packed, this translates into a decrease in the distance between neighboring micelles. An additional structural change might significantly contribute to the micelle size decrease. The saturation of negative charges inside the micelles enables new hydrophobic contacts and a closer packing between single casein monomers.[47,48] This leads to a higher dissociation volume of the micelle as high pressure experiments have

revealed.[49,50] This could also change the casein micelles' dimensions. A more homogeneous and compact casein micelle form was recently found after high pressure treatment.[11] It was proposed that the compaction is caused by a pressure-induced increase in the calcium concentration and a subsequent enhancement of the hydrophobic contacts.

E) Solution Casting

Besides spin coating and Langmuir Blodgett techniques, solution casting is an alternative method of preparing biofims for GISAXS investigations. It has the advantage that the solution casting technique enables the preparation of a gradient film. However, solution casting, which is driven by the evaporation of solvent via the liquid–gas interface, is a time-consuming process. It also produces thick films compared to the two techniques mentioned above.

Spin-coating and Langmuir Blodgett processes offer the possibility of thin film preparation. During the spin coating process, a solution drop is spinned leaving a layer on the substrate which thins due to fluid flow. This procedure initiates nonequillibrium structures and enlarges the range of accessible structures. In the Langmuir Blodgett technique, compressed protein monolayers are transferred from a subphase surface to the substrate. During protein monolayer formation the acting surface tension has the same magnitude as the dominant forces in protein folding, which leads to the risk of protein denaturation [51]. Modifications of the method enable the structures to be maintained, resulting in highly ordered protein nanotemplates which accelerate nucleation and crystal growth [52]. For caseins however, the spin coating technique was previously used for thin film preparations [25,26]. It has been shown that moderate pressures acting during the spinning process do not affect the casein micelle integrity and the results match in good approximation with those presented here.

Conclusions

The presented work shows the variation of casein components within a calcium gradient film prepared by solution casting. It compliments previous GISAXS studies on thin casein films, prepared by the spin coating technique by the use of an alternative film preparation technique. This allows much larger film thicknesses to be achieved with a superimposed gradient. For data analysis a form-factor model was used factoring in log-normal distributed polydispersity of the sample. The results confirm the growth of casein mini-micelle sizes and a decrease in the diameter of casein micelles with an increasing calcium concentration. Additionally, a shoulder in the scattering curves at 1 nm^{-1} was resolved which may arise from nano-sized calcium phosphate particles. The sizes of the particles are comparable with previous EM results. Within the calcium gradient no size variation of the calcium phosphate particles was observed.

The high real-space resolution, achieved by focusing the beam with a diameter of 1 μm onto the sample, allows local structures within heterogeneous films to be probed, such as gradient films prepared by solution casting. The calcium gradient replaces a huge number of individual samples and allows for combinatorial studies by varying one parameter – in this case the calcium concentration – in a controlled way and by scanning using a micrometer sized beam on one single representative sample. Surface scattering conditions were achieved by height scans at a fixed position in the gradient film. The described μGISAXS method is suited for the investigation of heterogeneous films such as gradient films.

Acknowledgements

A. Tolkach, E. Metwalli and U. Kulozik are gratefully acknowledged for stimulating discussions and supplying the casein. The assistance of R. Davies and J. Swann in proof reading and correcting the manuscript is appreciated. We obtain financial support by the FP6 SAXIER grant and DFG (MU 1487/8-1) within the priority program SPP1259.

captions to figures

Figure 1: Schematic representation of calcium gradient film preparation technique; 1) casein suspension with increasing amounts of calcium from left to right; 2) sequential loading of micropipette with solution; 3) gradient preparation by slowly releasing solution while moving of pipette along the glass slide; 4) schematic view of the scattering geometry: α_i denotes the angle between the incident beam k and the sample surface, α_f – the corresponding exit angle and ψ – the diffuse scattering angle. q_y and q_z are the components of the scattering vector q.

Figure 2: Detector intensity signal as a function of exit angle αf and out of plane angle ψ at different sample heights. The associated schematic representations of the scattering, with the incoming (—), transmitted and reflected (---) and scattered beam (—) are shown below. The color in the upper legend represents scattered intensity values.

Figure 3: (a) Double logarithmic plot of horizontal line cuts taken from the 2d GISAXS signal. Calcium concentration increases from the bottom to the top. The solid lines correspond to model fits, contained within the experimental error.

Figure 4: Fitted mean sizes for casein micelles (circle), casein submicelles (rectangle), and micellar calcium phosphate particles (rhombohedra) at varying calcium concentrations.

Figure 5: Size distribution contour plot of casein compounds along the calcium gradient; micellar calcium phosphate (left), casein mini-micelles (middle), and casein micelle (right).

Figure 6: Variation in size distribution at 0 mM and 60 mM calcium. (left) micellar calcium phosphate, (middle) casein mini-micelles, (right) casein micelles.

figures

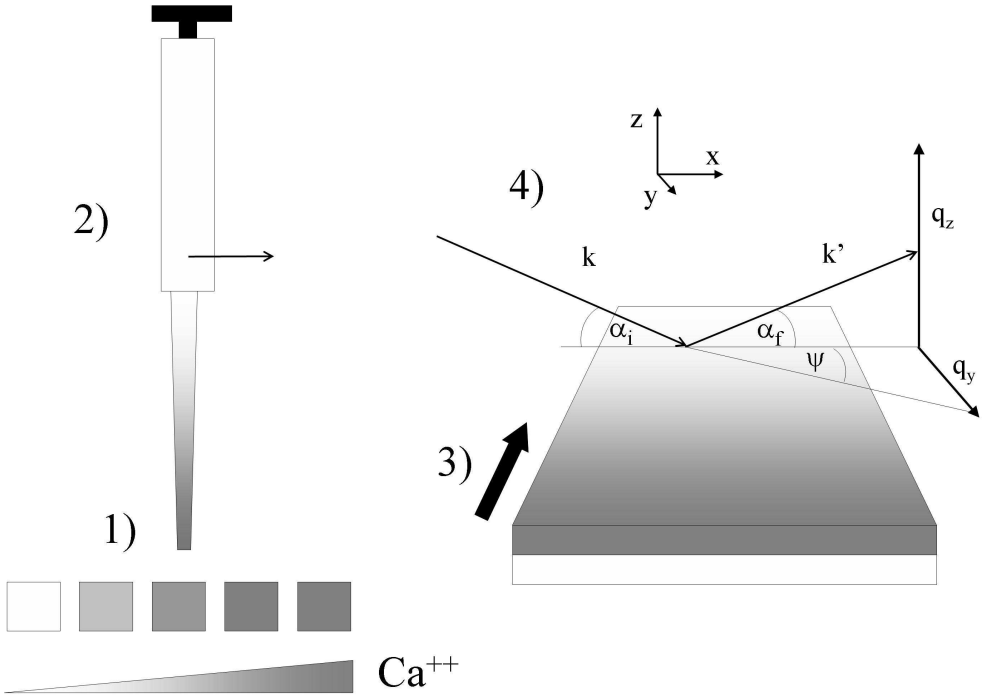

Figure 1

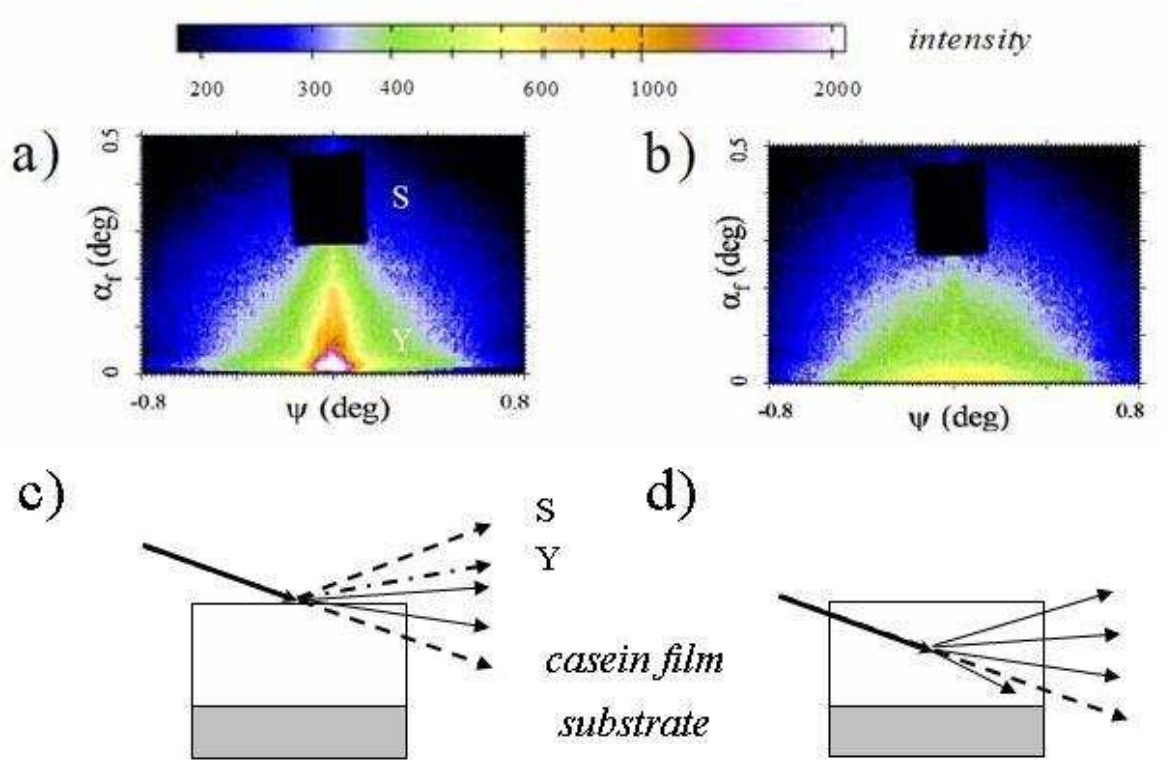
intensity
200
300
400
600
1000
2000
a)
b)
S
Y
α_f (deg)
0.5
0
-0.8
ψ (deg)
0.8
c)
d)
S
Y
casein film
substrate

Figure 2

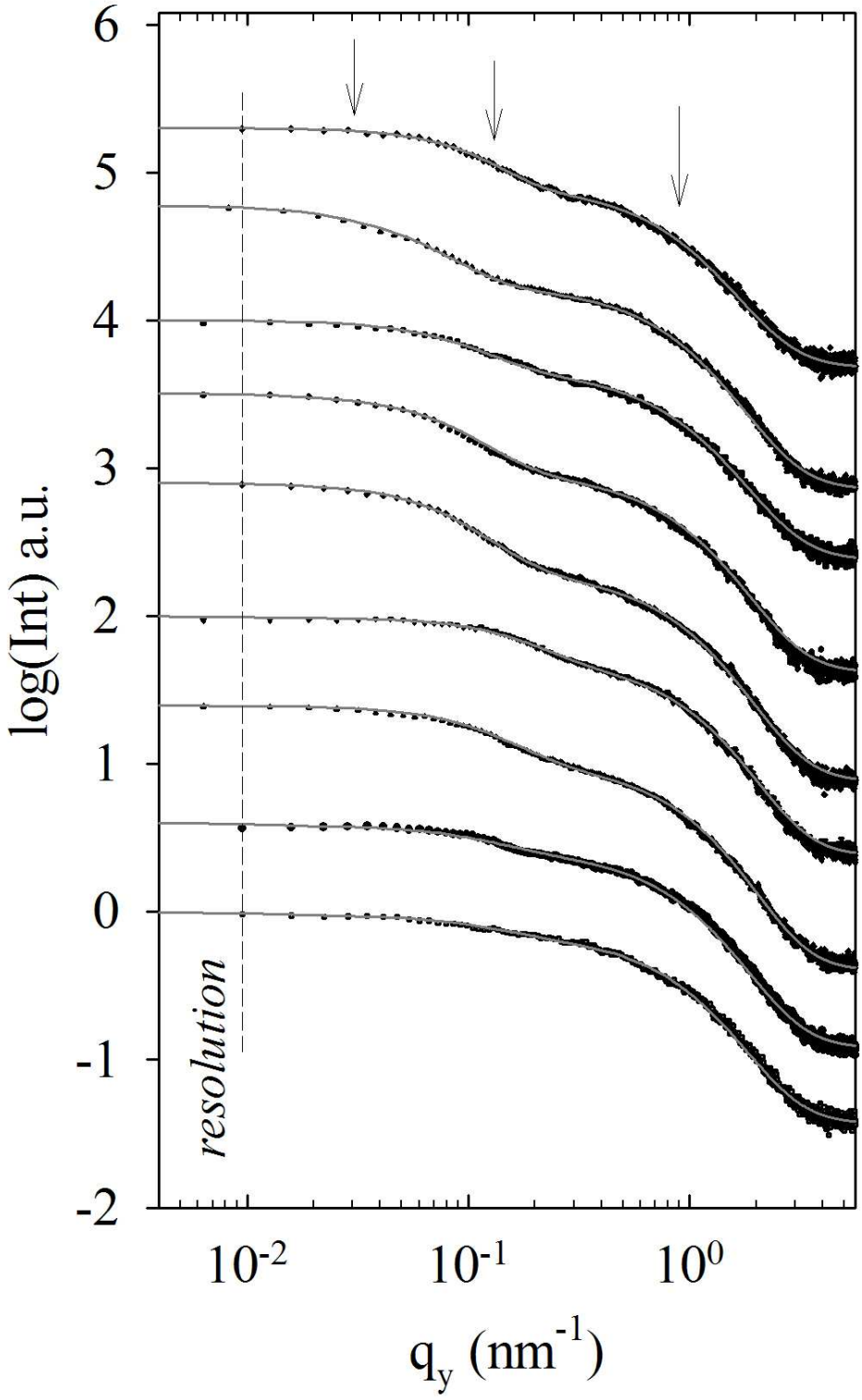

Figure 3

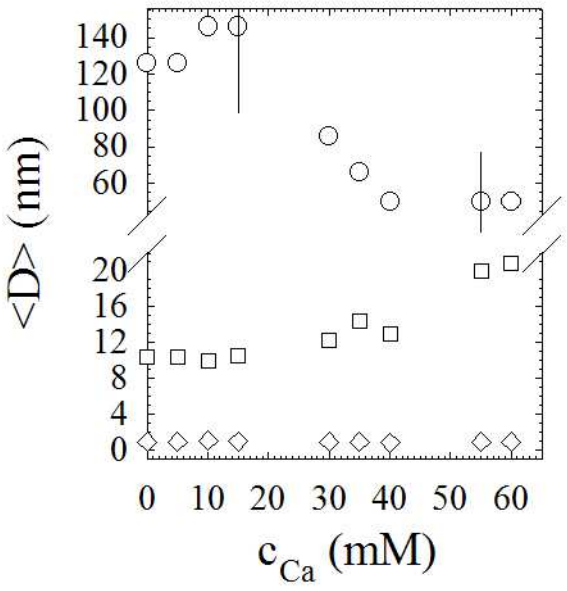

Figure 4

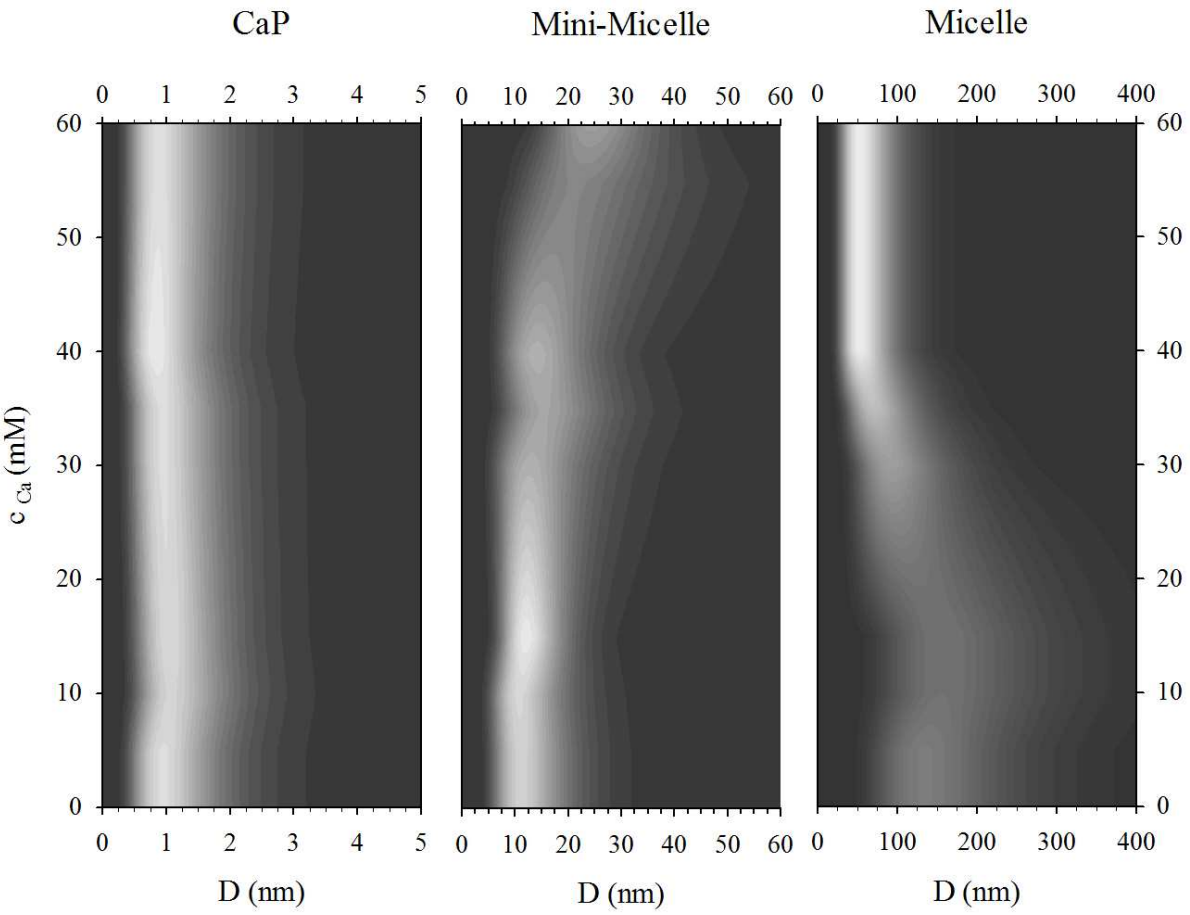

Figure 5

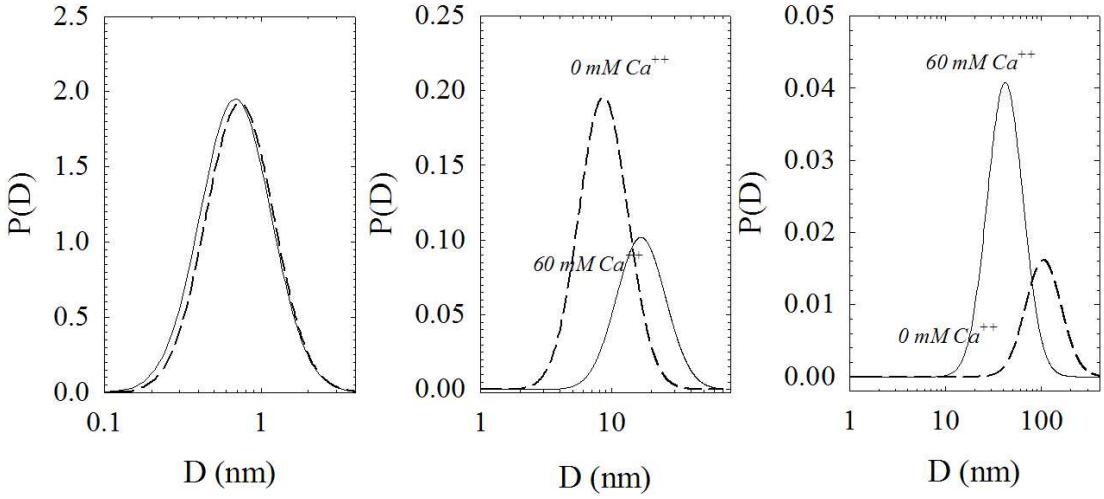

Figure 6

collected references

[1] C. G. de Kruif, *J. Dairy Sci.* 1998, 81, 3019-3028
[2] R. Tuinier, C. G. de Kruif, *Journal of Chemical Physics* 2002, 177, 1290-1295
[3] J. E. O'Connell, V. Ya. Grinberg, C. G. de Kruif, *Journal of Colloid and Interface Science* 2003, 258, 33-39
[4] S. R. Euston, D. S. Horne, *Food Hydrocolloids* 2005, 19, 379-386
[5] R. Boisgard, E. Chanat, F. Lavialle, A. Pauloin, *Livest. Prod. Sci.* 2001, 70, 49-61
[6] D. J. McMahon, W. R. McManus, *J. Dairy Sci.* 1998, 81, 2985-2993
[7] P. Walstra, *Int. Dairy J.* 1999, 9, 189-192
[8] C. Holt, C. G. de Kruif, R. Tuinier, P.A. Timmins, *Colloids Surf A* 2003, 213, 275-284
[9] D. S. Horne, Curr. Opinion in Colloid and Interface Sci. 2006, 11, 148-153
[10] D. G. Dalgleish, P. A. Spagnuolo, H. G. Goff, *Int. Dairy J.* 2004, 14, 1025-1031
[11] R. Gebhardt, W. Doster, J. Friedrich, U. Kulozik, *Eur. Biophys. J.* 2006, 35, 503-509
[12] C. Holt, D. S. Horne, *Netherlands Milk and Dairy Journal* 1996, 50, 85-111
[13] P. Walstra, *J. Dairy Sci.* 1990, 73, 1965-1979
[14] M. C. Neville, *Journal of Mammary Gland Biology and Neoplasia* 2005,10, 119-128
[15] D. B. Shennan, M. Peaker *Physiological Review* 2000, 80, 3, 925-951
[16] C. Holt, L. Sawyer, *J. Chem. Soc. Faraday. Trans.* 1993, 89, 2683-2692
[17] C. G. de Kruif, C. Holt *In: Fox PF, McSweeney P. (Eds) Advanced Dairy Chemistry, vol 1: proteins, Kluwer/Plenum, New York* 2003, 233-276
[18] C. Holt, *In* Developments in Dairy Chemistry. P. F. Fox, editor. Chapman and Hall, London 1997
[19] C. Holt, *Eur. Biophys. J.* 2004, 33, 421-434
[20] P. Müller-Buschbaum, *Annal. Bioanal. Chem*. 2003, 376, 3-10
[21] S. Regnault, M. Thiebaud, E. Dumay, J. C. Cheftel, *Int. Dairy J.* 2004, 14, 55–68
[22] E. Pechkova, S.V. Roth, M. Burghammer, D. Fontani, C. Riekel, C. Nicolini, *J. Synchrotron Rad.* 2005, 713-716
[23] C. Nicolini, E. Pechkova, *J. Cell. Biochem.* 2006, 97, 544-552
[24] E. Pechkova, C. Nicolini, , *J. Cell. Biochem.* 2006, 97, 553-560
[25] P. Müller-Buschbaum, R. Gebhardt, E. Maurer, E. Bauer, R. Gehrke, W. Doster, *Biomacromolecules* 2006, 7, 1773-1780
[26] P. Müller-Buschbaum, R. Gebhardt, S. V. Roth, E. Metwalli, W. Doster, *Biophys. J.* 2007, 93, 960-968
[27] M. L. Green, R. J. Marshall, *J. Dairy Res*. 1977, 44, 521-531
[28] D. G. Dalgleish, *J. Dairy Res.* 1983, 50, 331-340
[29] S. H. C. Lin, S. L. Leong, R. K. Dewan, V. A. Bloomfield, C. V. Morr, *Biochemistry* 1972, 11, 1818-1821
[30] R. J. Baxter, *J. Chem. Phys*. 1968, 49, 2770-2774
[31] A. Tolkach, U. Kulozik, *Journal of Food Engineering* 2005, 67, 13-20
[32] Y. Yoneda, *Phys. Rev.* 1963, 131, 2010
[33] T. Salditt, T. H. Metzger, J. Peisl, B. Reinker, M. Moske, K. Samwer, *Europhys. Lett.* 1995, 32, 331
[34] C. Riekel, *Rep. Prog. Phys*. 2000, 63, 233-262
[35] S. V. Roth, M. Burghammer, C. Riekel, P. Müller-Buschbaum, A. Diethert, P. Panagiotou, H. Walter, *Appl. Phys. Lett.* 2003, 82, 1935-1937
[36] A. Hammersley, In http://www.esrf.fr/comuting/scientific/FIT2D/
[37] R. Bauer, M. Hansen, S. Hansen, L. Øgendal, S. Lomholt, K. Qvist, D. Horne, *J. Chem. Phys.* 1995, 103,7
[38] B. Chu, Z. Zhou, G. Wu, H. M. Farrell, *J. Colloid Interface Sci.* 1995, 170, 102-112

[39] F. Pignon, G. Belina, T. Narayanan, X. Paubel, A. Magnin, G. Gesan Guiziou, *J. Chem. Phys.* 2004, 121, 8138
[40] S. Marchin, J-L. Putaux, F. Pignon, J. Léonil, *J. Chem. Phys.* 2007, 126, 045101
[41] S. Hansen, R. Bauer, S. B. Lomholt, K. Bruun Qvist, S. V. Pedersen, K. Mortensen, *Eur. Biophys. J.* 1996, 24, 143-147
[42] T. C. A. McGann, W. Buchheim, R. D. Kearney, T Richardson, *Biochim. Biophys. Acta* 1983, 760, 415-420
[43] F. Gaucheron, *Reprod. Nutr. Dev.* 2005, 45, 473-483
[44] T. Aoki, T. Uehara, A. Yonemasu, M. Zin El-Din, *J. Agric. Food Chem.* 1996, 44, 1230-1234
[45] D. F. Waugh, P. H. von Hippel, *J. Am. Chem. Soc.* 1956, 78, 4576 – 4582
[46] A. Thurn, W. Burchard, R. Niki, *Colloid Polym. Sci.* 1987, 265, 653-666
[47] D. S. Horne, *Int. Dairy J.* 1998, 8, 171-177
[48] D. S. Horne, *Colloids Surf.* A. 2003, 213, 255-263
[49] R. Gebhardt, *Ph.D. Thesis, TU Munich, Germany* 2005
[50] R. Gebhardt , W. Doster , U. Kulozik, *Braz. J. Med. Biol. Res.* 2005, 38:1209–1214
[51] C. Nicolini, *Trends Biotechnol*. 1997, 15, 395-401
[52] E. Pechkova, C. Nicolini. *Trends Biotechnol*. 2004, 22, 117-122

text for table of contents

Casein micelles in a calcium gradient film explored for the first time using microbeam gracing incident small-angle X-ray scattering (μGISAXS). The study allows the continuous investigation of the calcium effect over a broad range of length scales.

graphic for table of contents